ELSEVIER

Materials Science and Engineering A 431 (2006) 118–122

MATERIALS SCIENCE & ENGINEERING A

www.elsevier.com/locate/msea

Properties of pulse plated ZnSe films

K.R. Murali [a,*], M. Balasubramanian [b]

[a] *Electrochemical Materials Science Division, Central Electrochemical Research Institute, Karaikudi-630006, India*
[b] *Department of Physics, Rajus' College, Rajapalayam, India*

Received 26 March 2006; accepted 23 May 2006

Abstract

ZnSe thin films were pulse plated on titanium and tin oxide substrates maintained at room temperature from the precursors. The films exhibited cubic structure. Optical band gap of 2.70 eV was obtained. XPS measurements indicated the formation of ZnSe. AFM studies indicated that the grain size decreased as the duty cycle decreased. Hot probe measurements indicated films to be n-type. Luminescence emission was observed at 675 nm for an excitation of 450 nm.

Keywords: ZnSe; Semiconductor; Thin film; Electrodeposition; Pulse plating

1. Introduction

Zinc selenide is one of the most interesting binary wideband gap II–VI semiconductors, which has potential applications in the fabrication of blue light emitting diodes, blue lasers and as window material in the field of photo-voltaics [1]. Several techniques like vacuum evaporation [2], chemical bath deposition [3], spray pyrolysis [4], pulse electrodeposition [5], electrodeposition [1,6] and pulsed laser deposition [7] have been employed for the depostion of ZnSe films. All the reports have presented results on electrical, optical and photo-activity. In this work, results on structural, optical and luminescent properties of brush plated ZnSe films are presented. To our knowledge this is the first report on pulse plated ZnSe films. Generally in electrodeposition techniques for producing a metal or compound, a driving force in the form of potential or current is applied to the electrode. Either of these can be used as a variable as in the case of continuous electrodeposition. But modern electronics allows one to make use of these parameters as a function of time. This permits a number of possible ways of varying the conditions.

Four varaiable parameters are of primary importance in pulse plating. They are:

peak current density, i_p;
average current density, i_a;
ON time; and
OFF time.

The sum of the ON and OFF times constitute one pulse cycle. The duty cycle is defined as follows:

$$\text{duty cycle} = \frac{\text{ON time}}{\text{ON time} + \text{OFF time}} \times 100\%$$

A duty cycle of 100% corresponds to continuous plating because OFF time is zero.

In practice, pulse plating usually involves a duty cycle of 5% or greater. The average current density under pulse plating conditions is defined as:

$$I_a = \text{peak current density} \times \text{duty cycle}$$
$$I_a = i_p \times \text{duty cycle}$$

During ON time the concentration of the metal ions to be deposited is reduced within a certain distance from the cathode surface. This so called diffusion layer pulsates with the same frequency as the applied pulse current. Its thickness is also related to i_p but reaches a limiting value governed primarily by the diffusion coefficient of the metal ions. During the OFF time the concentration of the metal ions builds up again by diffusion from the bulk electrolyte and will reach the equilibrium concentration of the bulk electrolyte if enough time is allowed.

These variables results in two important characteristic features of pulse plating which make it useful for alloy plating as

* Corresponding author. Tel.: +91 4565227550; fax: +91 4565227553.
E-mail address: muraliramkrish@gmail.com (K.R. Murali).

0921-5093/$ – see front matter © 2006 Published by Elsevier B.V.
doi:10.1016/j.msea.2006.05.123

well as property changes as mentioned earlier. They are:

(i) Very high instantaneous current densities and hence very high negative potentials can be reached. The high overpotential causes a shift in the ratio of the rates of reactions with different kinetics. This high over potential associated with the high pulse current density greatly influences the nucleation rate because a high energy is available for the formation of new nuclei.
(ii) The second characteristic feature is the influence of the OFF time during which important adsorption and desorption phenomena as well as recrystallization of the deposit occurs.

2. Experimental

Zinc selenide thin films were deposited on titanium and conducting glass substrates by the pulse plating technique at different duty cycles in the range of 6–50%, using 20 ml of 0.25 M zinc sulphate and 2 ml of 0.01 M selenium dioxide at a current density of 100 mA cm^{-2}. The duration of deposition was 30 min. The thickness of the films, was estimated by gravimetry and it was found to vary between 1.0 and 2.5 μm according to the duty cycle. Structural characterization was carried out by X-ray diffraction (XRD) studies using Cu Kα radiation. Employing a molecular imaging systems atomic force microscope, morphological studies were carried out. Optical studies were made on the films deposited on conducting glass substrates with a Hitachi UV–vis-NIR spectrophotometer. XPS studies were made using ESCALAB. Laser Raman studies were made using Renishaw LABRAM system. Luminescence emission spectra of the samples were recorded at room temperature using a mercury lamp source. The excitation wavelength was 450 nm and the emission was recorded in the wavelength range 550–720 nm.

3. Results and discussion

XRD patterns of the films deposited at different duty cycles in the range 6–50% are presented in Fig. 1. It is observed that the films exhibit cubic structure with peaks corresponding to (1 1 1), (2 2 0) and (3 1 1) orientations. Two peaks corresponding to the substrate Ti are observed for the films deposited at low duty cycles, as the duty cycle increases, the intensity of the peak corresponding to (1 1 1) orientation also increased, indicating the preferential orientation of the films in this direction, the peaks corresponding to titanium are also absent for higher duty cycles due to the increased thickness of the films deposited at higher duty cycles. The thickness of the films increases from 1.0 to 2.5 μm as the duty cycle increases, due to the availability a large flux of ions for deposition at every new pulse at higher duty cycles. At lower duty cycle, since the pulse is ON only for a short period, only a small flux of ions are available for deposition, moreover due to the application of a pulse of high current density for a short duration, the crystallite size is also small for lower duty cycles. This is evident from the broad peaks for the films deposited at lower duty cycles. As the duty cycle increases, the peaks become sharper due to improved crystallinity. The crystallite size estimated by using Scherrer's equation[8], was

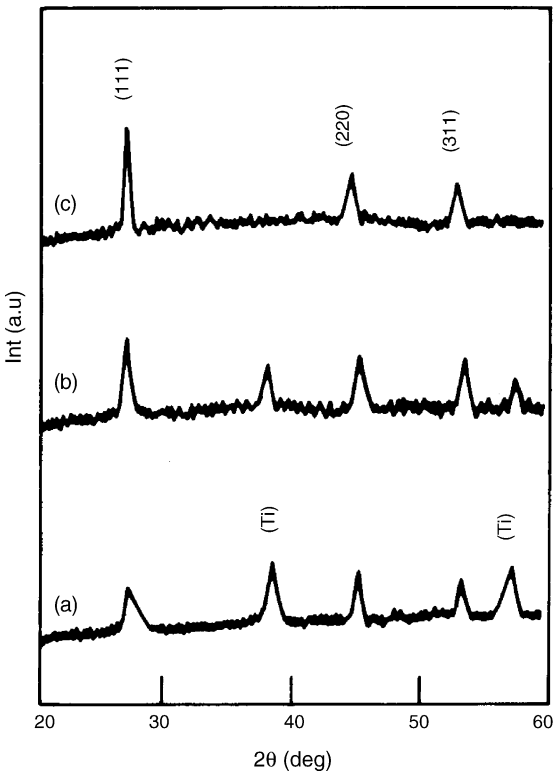

Fig. 1. X-ray diffraction pattern of ZnSe films deposited at different duty cycles: (a) 6%; (b) 25%; (c) 50%.

found to increase from 15 to 50 nm as the duty cycle increases. Composition of the films before and after heat treatment were estimated by EDAX measurements and it was found to be 49.8% Zn and 50.2% Se for the as deposited films.

Optical absorption studies were made on the films deposited on conducting glass substrates in the wavelength range 300–900 nm at room temperature to ascertain the nature of the band gap. For allowed direct transitions, the absorption coefficient 'α', near the absorption edge is given by [9]:

$$\alpha = (A/h\nu)(h\nu - E_g)^{1/2} \quad (1)$$

where h is the Planck's constant, ν the frequency of the incident light and A is related to the effective mass of holes and electrons. A plot of $(\alpha h\nu)^2$ versus $h\nu$ (Fig. 2) for the films deposited at a duty cycle of 50% was linear, indicating the direct band nature of the films. Band gap obtained by extrapolating the linear portion was 2.7 eV. The band gap was found to increase up to 3.1 eV as the duty cycle decreased, due to quantum confinement.

To examine the chemical composition of the films, the XPS spectra of the ZnSe films grown at different duty cycle, were measured and as a representative case results are reported for the film deposited at 90 °C (Fig. 3). The XPS spectra of the films exhibit the binding energies of the Zn($2p_{3/2}$) and Se($3d_{5/2}$and $3d_{3/2}$) level. As shown in Fig. 4a, the peak energy levels associated with Zn($2p_{3/2}$) appeared at about 1022 eV, which is in good agreement with literature [10]. These findings are characteristic of the Zn in ZnSe and are in good agreement with literature [10]. Fig. 4b shows the binding energies of the Se($3d_{5/2}$ and $3d_{3/2}$) levels at 53.9 and 59.2 eV, respectively. In order to make

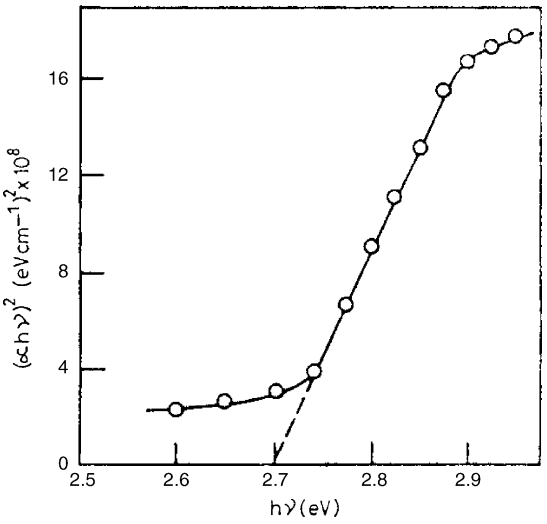

Fig. 2. $(\alpha h\nu)^2$ vs. $h\nu$ plot for ZnSe film deposited at a duty cycle of 50%.

a compositional analysis in the whole thickness of the film, XPS measurements were performed on films submitted to sputtering at different times. The study indicates an increasing Zn/Se atomic ratio with depth, varying from 0.97 at the surface to 1.5

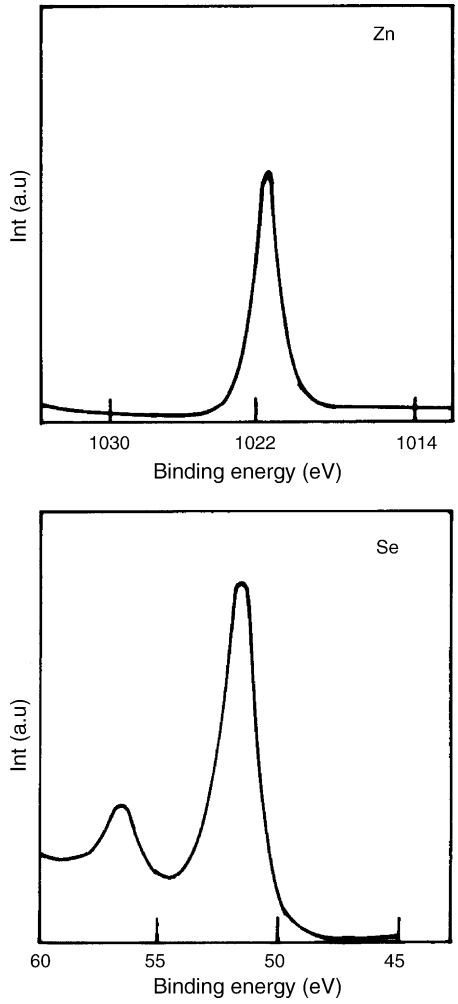

Fig. 3. XPS spectra of ZnSe film deposited at a duty cycle of 50%.

close to the film substrate interface. Similar type of increase in Zn/Se ratio with depth was observed for chemical bath deposited ZnSe films [10].

Atomic force microscope images of the films deposited at different duty cycles is shown in Fig. 4. The best ordering is observed for the films deposited at a duty cycle of 6% (Fig. 4a). Larger grain size was observed for the films deposited at higher duty cycles (Fig. 4b and c), these results are consistent with the XRD results.

Laser Raman studies were made using 633 nm laser radiation. The films deposited at lower duty cycles indicated a broad and small peak at 252 cm^{-1} (Fig. 5). This peak corresponds to the longitudinal optical (LO) phonons in ZnSe. As the duty cycle increased, the peaks became sharper and increase in height, this is due to the improved crystallinity of the films deposited at higher duty cycle supported by X-ray diffraction results. This is similar to the results obtained with photochemically deposited ZnSe films [11]. The spectra display a typical multiphonon Raman Process, up to the third order LO phonons are observed, which reveals the strong dominance of the Frohlich electron–phonon interaction [12], which is the main mechanism of the coupling between carriers and LO phonons in polar semiconductors.

The semiconductor electrolyte interfacial region is endowed with electrical heterogeneity on account of the existence of the depletion layer on the semiconductor side and a diffused double layer on the solution side. The overall capacitance of this region of photoelectric activity is made up of two distinct contributions from these space charge regions existing on either side of the interface. In view of the relatively much lower carrier density in the depletion layer, the experimentally measured capacitance of the semiconductor-electrolyte interfacial region is attributed to the semiconductor alone [13,14]. The charge distribution in the depletion layer is altered when the semiconductor potential is varied.

The semiconductor capacitance thus depends on the electrode potential. This is expressed in terms of a Mott–Schottky relationship [15–18].

$$\frac{1}{C^2} = \frac{2}{qN_A}\varepsilon\varepsilon_o\left(\frac{V - V_{fb} - kT}{q}\right) \quad (2)$$

where N_A is the acceptor density, ε and ε_o are the dielectric constants of the semiconductor and the vacuum, respectively, q the electronic charge, V_{fb} the flat band potential, k the Boltzmann constant and T is the absolute temperature. According to this relation, $1/C^2$ versus V plots should be linear (Fig. 6). The data indicates the p-type nature of the electrode. Extrapolation of the straight line to the voltage axis yields a flat band potential of +0.70 V (SCE). The charge carrier density, N_A was estimated from the slope of the plot and is 6.95×10^{18} cm^{-3}.

Photoluminescence (PL) spectra were recorded at room temperature using an excitation wavelength of 450 nm. The spectra peaks at 675 nm (Fig. 7) and the PL intensity was found to increase with duty cycle. The PL emission from the undoped ZnSe has been attributed to the presence of native defects like zinc and selenium vacancies or interstitials, which are likely

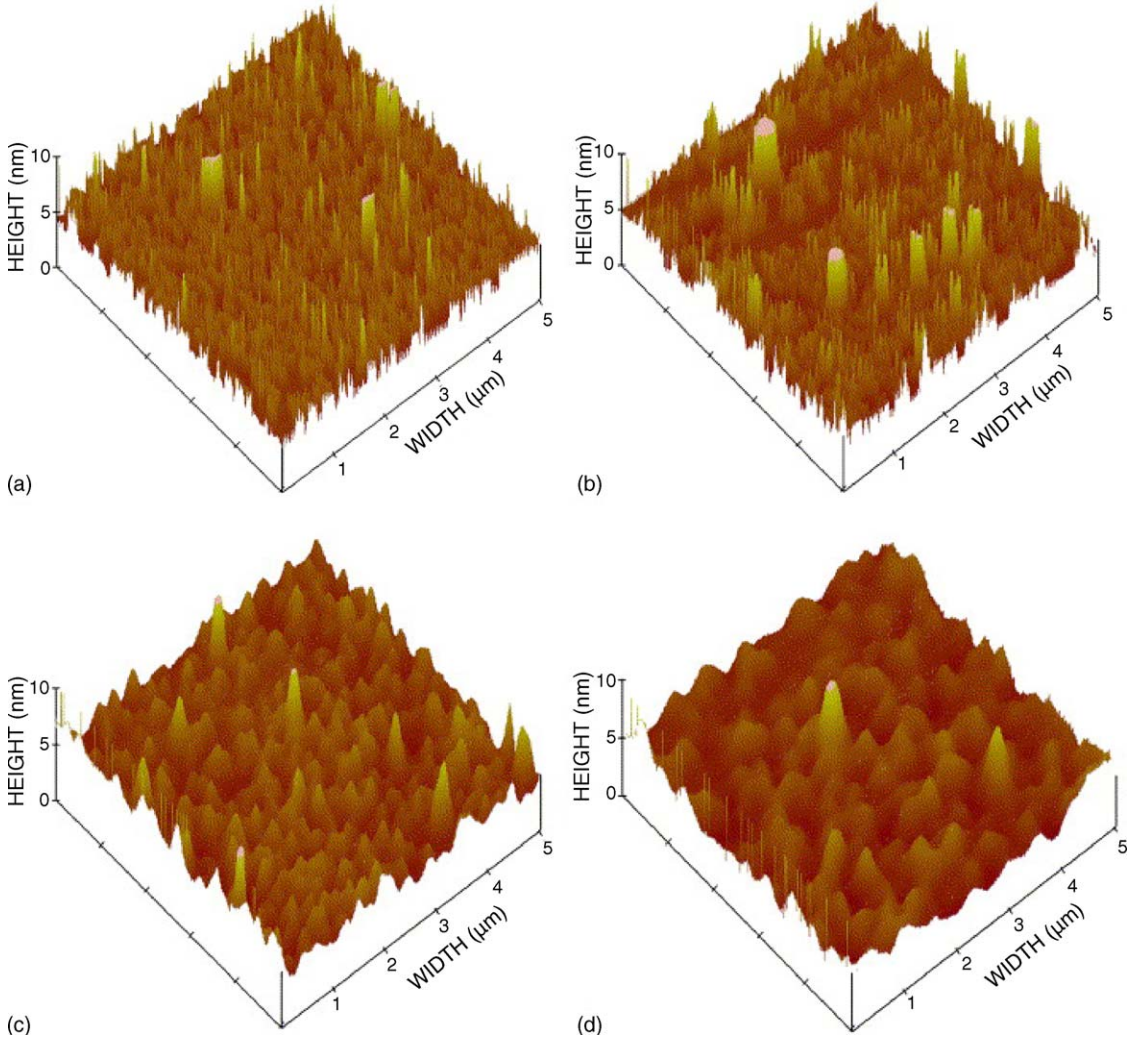

Fig. 4. AFM images of ZnSe films deposited at different duty cycles: (a) 6%; (b) 25%; (c) 50%.

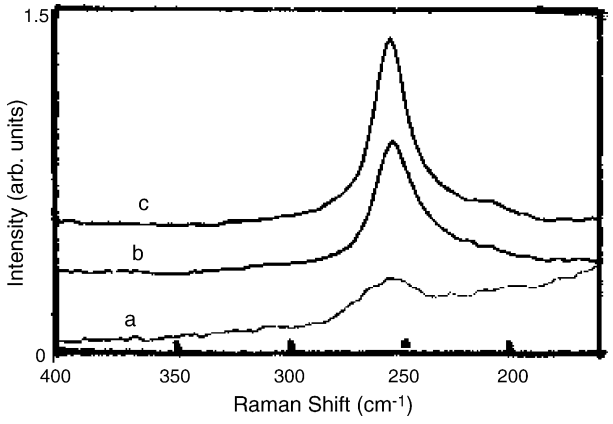

Fig. 5. Raman spectrum of ZnSe films deposited at different duty cycles: (a) 6%; (b) 25%; (c) 40%; (d) 50%.

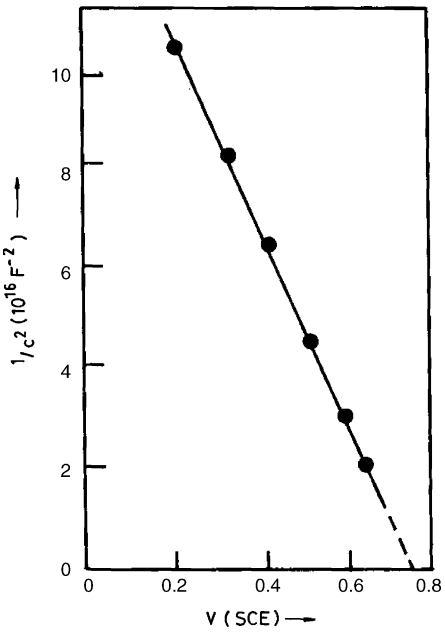

Fig. 6. Mott Schottky plot of ZnSe film deposited at a duty cycle of 50%.

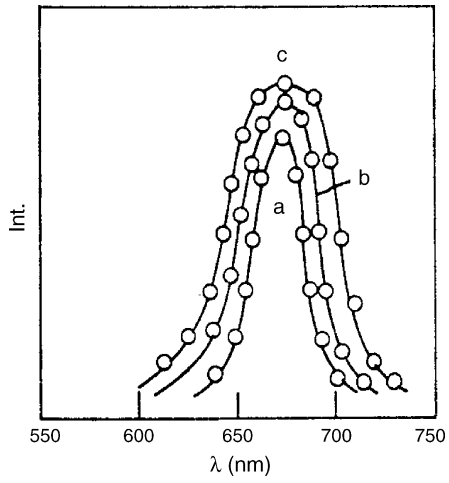

Fig. 7. Photoluminescence spectra of ZnSe films deposited at different duty cycles (a) 6%; (b) 25%; (c) 50%.

to be introduced during the growth process [19]. Self-activated centers arising from complexes of zinc vacancies and shallow donors (selenium interstitials) would occur around 2.0 eV [20]. The emission band observed in the present case at 675 nm may be attributed to the above complex, since EDAX studies have indicated a slight excess of selenium.

4. Conclusions

The results of this investigation indicates that the simple and economical pulse plating technique can be employed for the preparation of luminescent ZnSe films. Further work is on to scale up the process for large area film deposition. This can be employed for the commercial production of large area films. Further improvement in the performance can be made by heat treatment steps as well as by in situ doping with copper or manganese.

References

[1] C. Natarajan, M. Sharon, C. Levy Clement, H. Nuemann Spallart, Thin Solid Films 118 (1994) 234.
[2] M. Ei Sheriff, F.S. Terra, S.A. Koelier, J. Mater. Sci. Mater. Electron. 7 (1996) 391.
[3] C.D. Lokhande, P.S. Patil, A. Ennari, H. Tributch, Appl. Surf. Sci. 123–124 (1998) 294.
[4] H.C. Baylere, S. Kose, V. Bilgin, Blue Laser Light Symp. (1998) 516.
[5] K.R. Murali, S. Chander, V.R. Srinivasan, V. Swaminathan, M. Balasubramanian, 197th Meeting of the Electrochemical Society, Toronto, USA, 2000, p. 504.
[6] C.B. Roy, D.K. Nandi, P.K. Mahapatra, Electrochim. Acta 31 (1986) 1227.
[7] T. Ganguli, B.L. Dashora, P. Bhattacharya, L.M. Kukreja, P. Bhatnagar, H.S. Rawat, M. Lal, A. Gupta, Diffus. Defect Data B 55 (1997) 59.
[8] A. Guiner, Theorie et Technique de la Radiocristallographie, Editions Dunod, Paris, 1969.
[9] J.I. Pankove, in: N. Holonyak (Ed.), Solid State Physical Electronics Series, Prentice Hall, Eaglewood Cliffs, NJ, USA, 1971.
[10] A.M. Chaparro, C. Maffiotte, M.T. Gutierrez, J. Herrero, Thin Solid Films 358 (2000) 22.
[11] R. Kumaresan, M. Ichimura, E. Arai, Thin Solid Films 414 (2002) 25.
[12] M. Cardona (Ed.), Topics in Applied Physics, Light Scattering in Solids I, vol. 8, Springer, Berlin, 1975.
[13] H. Gerischer, in: H. Evaing, D. Henderson, W. Jost (Eds.), Physical Chemistry, An Advanced Treatise, vol. 9A, Academic Press, 1970.
[14] R. Memming, in: A.J. Bard (Ed.), Electroanalytical Chemistry, vol. 11, M. Dekker, Inc., New York, 1979.
[15] F.R.F. Fan, A.J. Bard, J. Electrochem. Soc. 128 (1981) 945.
[16] G. Nagasubramanian, A.S. Gioda, A.J. Bard, J. Electrochem. Soc. 128 (1981) 2158.
[17] Kabir-ud-din, R.C. Owen, M.A. Fox, J. Phys. Chem. 85 (1981) 1679.
[18] S. Chandra, S.N. Sahu, Phys. Status Solidi A 89 (1985) 321.
[19] T. Yodo, R. Ueda, K. Morio, R. Yamasita, S. Tanaka, J. Appl. Phys. 68 (1990) 3212.
[20] F. Sokurai, K. Suto, S. Sanda, J. Nishizawa, J. Electrochem. Soc. 149 (2002) G100.